

Photo-thermal Effect for Localized Desorption of Primary Lymphocytes Arrayed on an Antibody/DNA-based Biochip

Loïc Leroy, Radoslaw Bombera, Elodie Engel, Roberto Calemczuk, Loïc Laplatine, Dieu-donné R. Baganizi, Patrice N. Marche, Yoann Roupioz, and Thierry Livache

Supplementary Information

Table of contents

Supplementary Information	1
1 General Reagents	1
2 Methods of Synthesis.....	2
2.1 DNA-biochip functionalization.....	2
2.2 Antibody-DNA conjugation.....	3
3 Experimental Procedures.....	3
3.1 Cell culture	3
3.2 Dissociation temperature measurement	3
3.3 SPRi/laser-induced desorption set-up	4
3.4 Fluidic reaction chamber	5
3.5 Experimental run	6
3.6 SPRi data analysis and images treatments	6
3.7 Images analysis for cell density quantification	6
3.8 Heat resistance of cells.....	7
4 References	8

1 General Reagents

Following reagents were purchased from Sigma-Aldrich (France): IgG from rabbit serum (IgG R), NaCl, NaOH, H₂SO₄, H₂O₂, Dimethyl Sulfoxide (DMSO), Tris (2-carboxyethyl) Phosphine Hydrochloride (TCEP), 1-Dodecanethiol, Phosphate Buffer Saline (PBS), Bovine Serum Albumin (BSA), Foetal Bovine Serum (FBS), Concanavalin A (ConA), Ethylenediaminetetraacetic acid (EDTA), RPMI-1640 culture medium and MgCl₂. NH₄HCO₃ and N,N-Dimethylformamide (DMF) were purchased from Fluka. Tris-HCl (Tris(hydroxymethyl) aminomethane) as well as the cross-linker SM(PEG)₁₂ (succinimidyl-[(N-maleimidopropionamido)-dodecaethyleneglycol) were furnished by Interchim (France). Pyrrole was purchased from Tokyo Casei (Japan). Monoclonal rat anti-mouse CD19 (clone: 1D3) and monoclonal rat anti-mouse CD90 (clone: G7) were purchased from BD Biosciences (France). Monoclonal mouse IgG anti-HcB domain was kindly provided

by L. Bellanger (CEA/Institut de Biologie Environnementale et Biotechnologie IBEB, France). All chemicals were used without further purification. The oligonucleotide sequences were all purchased from Eurogentec (France) and are listed in Table 1. The probe oligonucleotides (Zip1, Zip2, R) bearing originally a primary amine group at 5' end have been covalently coupled to pyrrole moiety as previously described with proteins.^{1,2}

Name	Sequence (5'→3')
Probes	
Zip1	pyrrole-(T ₁₀)-GACCGGTATGCGACCTGGTATGCG
Zip2	pyrrole-(T ₁₀)-GACCATCGTGCGGGTAGGTAGACC
Zip3	pyrrole-(T ₁₀)-TGCGATCGCAGCGGTAACCTGACC
R	pyrrole-(T ₁₀)-TGGAGCTGCTGGCGT
Complementary stands	
Zip1*	CGCATAACCAGGTTCGCATACCGGTC
Zip2*	GGTCTACCTACCCGCACGATGGTC
Intermediate strands	
Zip1*-ZipI	TACCTTCG-GAATTC-ACTCGCACCGCATACCGGTCGCATACCGGTC
Zip2*-ZipII	GACAAGGT-CAGCTG-TAGGCAAGGGTCTACCTACCCGCACGATGGTC
Zip3*-ZipIII	CACTCACT-CCATGG-GCACTTGCGGTCAGGTTACCGCTGCGATCGCA
Targets	
ZipI*	GTGCGAGT-GAATTC-CGAAGGTA-(T ₁₀)-SH
ZipII*	CTTGCTA-CAGCTG-ACCTTGTC-(T ₁₀)-SH
ZipIII*	GCAAGTGC-CCATGG-AGTGAGTG-(T ₁₀)-SH

Table 1. Oligonucleotide sequences used in the study

*Complementary target strands are pointed out by an asterisk.

2 Methods of Synthesis

2.1 DNA-biochip functionalization

The DNA chips were prepared on a glass prism provided by Horiba Scientific-(France) coated with a gold layer of 45 nm of thickness. Prior to functionalization, the gold layer was cleaned with a *piranha* solution (2:1 H₂SO₄/H₂O₂ mixture (*Caution: piranha* solution is exothermic and strongly reacts with organics) and then immersed in 20 mM solution of 1-dodecanethiol in ethanol for ~30 min at room temperature. The surface was then rinsed with ethanol and deionized water (18.2 MΩ.cm). The DNA probe grafting was realized using electropolymerization method as previously described^{1,2}. For each probe, a solution containing 20 mM of pyrrole and 5'pyrrole-modified probe at 10 μM was prepared (in water supplemented with 30 % of acetonitrile, 20 % of DMSO, 0.5 % of glycerol and 0.1 M of LiClO₄). The probes were subsequently assembled on the gold surface by using a μ-pipette tip and the deposition realized by 2 V electric pulse of 100 ms. The DNA spots obtained with this method were ~800 μm in diameter and the density of oligonucleotide probe was estimated³ at ~ 10 pmol.cm⁻². The

DNA probes were spotted in few repetitions in order to cover the most of surface possible (at ~ 0.5 cm² per probe). Prepared chip was dried, stored at 4 °C and used within few days.

2.2 Antibody-DNA conjugation

DNA and IgG coupling was performed using the hetero-bifunctional cross-linker SM(PEG)₁₂. In the first step, the IgG underwent covalent coupling with SM(PEG)₁₂. An appropriate IgG was suspended at ~ 5 μ M in pH 7.4 PBS buffer and mixed with 100 molar excess of the cross-linker. The protein activation reaction was carried out for 1 h at room temperature. Reactive sample was consequently purified on NAP-5 column (GE Healthcare) previously equilibrated with PBE buffer (pH 6.8 PBS with 5 mM EDTA) in order to remove the excess of SM(PEG)₁₂. Purified eluate was concentrated using 30 kDa MWCO spin filter membranes (15 min, 15000 g) and suspended in PBE. The activated protein concentration was determined by 280 nm absorbance measurement. In parallel, thiolated oligonucleotides (E1* or P2* in table 1) suspended in deionised water (~ 50 μ M) were mixed with TCEP in order to reduce disulfide bonds possibly formed between thiolated DNA oligomers (TCEP at 5 mM of final concentration). The reduction reaction was run for 30 min at room temperature, followed by purification on NAP-5 column (elution with PBE) and concentration using 3 kDa MWCO membranes (15 min, 15000 g). The final concentration in PBE was assayed by 260 nm absorbance measurement.

Solutions of reduced DNA oligomer and maleimide activated protein were subsequently used for the final coupling reaction. Thus, 2-fold molar excess of the protein molecule was combined with the DNA strand and allowed to react overnight at room temperature. The reaction sample was then concentrated on 30 kDa MWCO spin filter (15 min, 15000 g) and the buffer was exchanged to pH 7.4 PBS. Unreacted proteins as well as the conjugation products were fractionated on an anion exchange column HiTrap^{HM} Q FF 1 mL (GE Healthcare). Species were eluted from the column at 1 mL/min NaCl gradient flow using pH 8.0, Tris-HCl 20 mM, NaCl 137 mM as starting buffer. Collected fractions were concentrated at 30 kDa MWCO membranes (15 min, 15000 g) and suspended in pH 7.4 PBS buffer. The DNA loading of the protein molecules was estimated using respectively 260 nm and 280 nm absorbance values of conjugation products.⁴

3 Experimental Procedures

3.1 Cell culture

Primary splenocytes were collected from an adult C57Bl/6 mouse Mouse splenocytes (C57Bl/6) (collaboration with The Institut Albert Bonniot, France). Directly after the removal of the spleen, cells were separated on a grid mesh and suspended in cell culture medium (RPMI). The cellular suspension was then centrifuged (5 min, 300 g) and incubated in a lysis buffer (8.3 g/L NH₄Cl, 0.8g/L NaHCO₃, 0.04 g/L EDTA) for 5 minutes to eliminate red blood cells. B and T lymphocyte mixture was washed in PBS and centrifuged again (5 min, 300 g). Cell pellet was resuspended in RPMI complemented with 10 % FBS, penicillin (50 μ g/mL) and streptomycin (50 μ g/mL). Concavalin A (ConA) was added at 2 μ g/mL in order to stimulate T lymphocytes proliferation. Cells were cultured for 24 to 72 h at 37°C in 95% humidity and 5% CO₂ environment (Forma Steri Cycle CO₂ Incubator, Thermo Scientific). Prior to injection in the microfluidic system, cells were centrifuged (5 min, 300 g) and suspended in PBS supplemented with 20% of N,N-dimethylformamide (DMF) (v/v) at the concentration of 3.0 – 5.0 10⁶ cells/mL. Cell viability was previously measured and shown to be maintained over 95 % within up to three hours of incubation in PBS supplemented with 20 % of DMF (v/v). In the particular case of our study, lymphocytes are suspended in the running buffer for a short time (less than one hour). Although DMF may alter cell morphology or growth, the effect is reversible as demonstrated by previous works.^{5,6,7} Such system may be thus successfully applied to cell sorting purposes.

3.2 Dissociation temperature measurement

We measured the dissociation temperature of the duplexes Zip1/Zip1* and Zip2/Zip2* (Zip1* and Zip2* are respectively the complementary sequences of Zip1 and Zip2). Gold-coated prisms (Horiba Scientific - GenOptics, France) were functionalized by polypyrrole electrospotting as described above (DNA-biochip functionalization). A minimum of four DNA spots per sequence were grafted to control experimental reproducibility. Every biochip had control electro-polymerized spots

of non-functionalized polypyrrole and a non-complementary DNA sequence Zip3 to verify the specificity of hybridization. All experiments were carried out on a homemade, temperature-regulated Surface Plasmon Resonance imaging (SPRi) system as described by Fiche and coworkers.⁸ The running buffer contained phosphate-buffered saline (PBS) with 20% of DMF (v/v). For hybridization, target DNA was added to the running buffer at a final concentration of 200 nM. Hybridization was carried out for 10 min at 23 °C with a flow rate of 50 μ L/min. Then, after 3 min of rinsing, a controlled temperature scan was performed at 2 °C/min up to 80 °C. Thus, we obtained non equilibrium thermal denaturation curves for all DNA spots on the prism. To determine the dissociation temperature (T_d), defined as the temperature with 50% of the initial hybridization signal on the DNA spots,^{9,10} SPRi denaturation curves were normalized to 1 and averaged over identical DNA spots. Figure 1 shows the dissociation curves obtained for the studied duplexes (Zip1/Zip1* and Zip2/Zip2*). T_d is equal to 63 ± 2 °C for Zip1/Zip1* and to 62 ± 2 °C for Zip2/Zip2*. For more detail on this experiment please report to Fuchs et al.¹¹

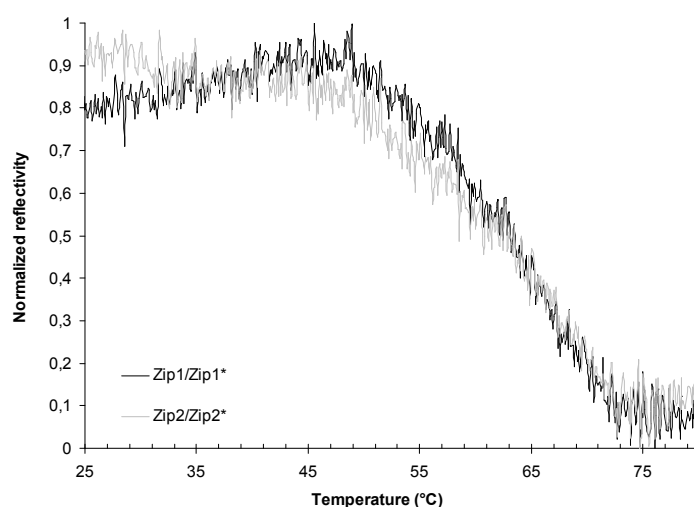


Figure 1. Denaturation curves for Zip1/Zip1* and Zip2/Zip2* obtained in PBS buffers 20% DMF.

3.3 SPRi/laser-induced desorption set-up

The experiments of photothermally induced desorption were carried out on a homemade SPRi system based on the well-known SPR Kretschmann configuration.¹² The gold-coated prism, functionalized by DNA probes, was placed in the optical detection system and was assembled with a microfluidic flow cell module (cf. 3.4) ensuring contact with biological medium. The incident illumination parallel beam ($\lambda = 660$ nm) was generated by a light-emitting diode (LED) associated with: -a pinhole (0.5 mm diameter); - an optical lens (focal length of 50 mm); -a linear polarizer adapted on a rotary optic mount. Under well-defined angle of incidence surface plasmons were excited. The reflected signal was recovered by a CCD camera (pike F-145B by Allied Vision Technologies GmbH) using a VZMTM 600i zoom imaging lens (Edmund optics) enabling real-time detection of the specific interactions (Figure 2 a). In order to produce the photothermal effect, a red-light laser beam was added to the classical optical system (Figure 2 b). Depending of experiments, two tunable power laser beams were used. In molecular experiments the beam was provided by a single 100mW 665nm laser diode focusable module. For cellular desorption experiments the beam was provided by a 500mW 653nm fiber-coupled laser system (Laser diode driver KS3-22312-103, BWT Beijing LTD) associated with a 10X/0.33 Olympus UPlan FLN objective. In both cases incidence angle and polarization of the heating laser were accurately adjusted in order to optimize the plasmon generation. This optimization was performed by measuring the minimum of the transmitted light with an Edmund optics handheld laser power meter. Laser spots were also accurately focused on the gold surface to minimize the laser spot size and maximize the reachable power density. By measuring the optical power losses and the effective size of laser spots on the gold surfaces, the maximum deposited surface power densities were respectively estimated at $1.9 \mu\text{W}/\mu\text{m}^2$ for the first setup and, $1 \mu\text{W}/\mu\text{m}^2$ for the second

one. Relative position of the focalized laser was commanded by external motors (step motor controller by Oriel 18011 mike controller) or with manual linear translation stages, enabling an accurate laser tracing on the prism surface. A microscope (Olympus BXFM) and appropriate objective (10X/0.33 Olympus UPlanFLN and X4/0,1 Edmund Micro plan), placed above the prism, allowed to visualize capture-release steps by classical reflection microscopy. Acquisitions were performed with an Infinity2-3C, Lumenera camera. To enable the laser beam localization the illumination light of the microscope was reduced nearly at the minimum value. Despite the high surface density of the laser beam as it was achieved over the full reflection angle, the intensity of transmitted light was very small (a few μW).

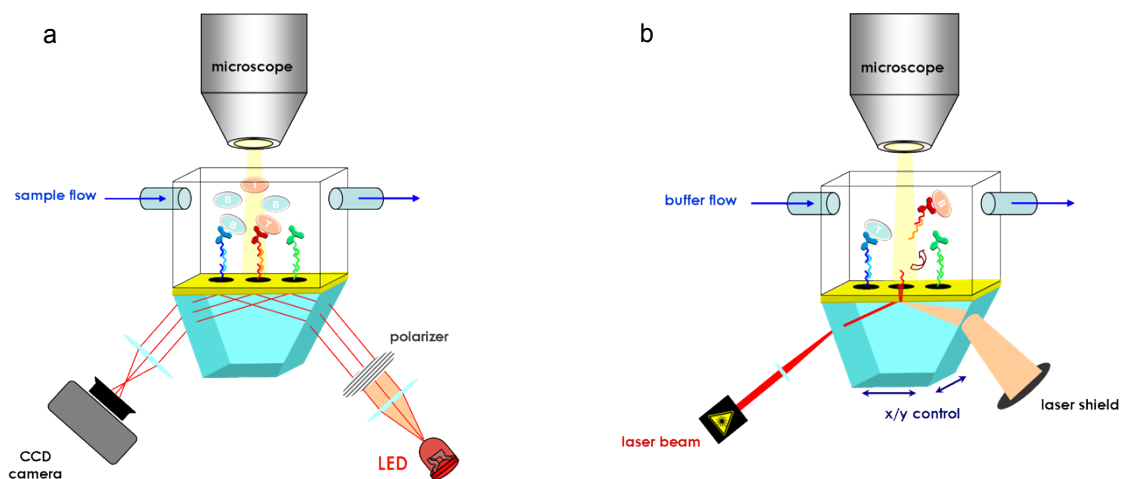


Figure 2. General scheme of the instrumental set-up used in the experiments of laser-induced desorption. a) SPR Imaging mode: real-time monitoring of biochip molecular assembly construction and cell capture/release steps. b) Lasing mode: photo-thermal desorption of species induced by a laser beam.

3.4 Fluidic reaction chamber

The reaction chamber consisted of a rectangular with rounded ends shape reactor of 140 μm of thickness and 9 mm of width in the working area (Figure 3). The length between inlet and outlet is 15 mm. Observations and treatments were performed in a 9x9 mm² central part of the prism.

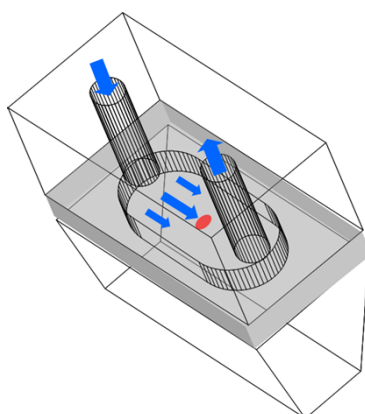


Figure 3. Illustration of the microfluidic setup.

The fluidic is completed by a 200 μL injection loop, a 50 mL syringe pump (A-99, razel Scientific Instruments Inc.) and PEEK/polyethylene tubings (ID = 760 μm).

3.5 Experimental run

Prior to the assay, DNA biochip was cleaned in an ultrasonic water bath (1-2 min). The DNA-biochip was then assembled in the microfluidic device. The required steps to convert the DNA-biochip into an antibody array were performed on chip under fluidic conditions at 20 μ L/min flow rate. First the DNA-biochip surface was blocked by injection of bovine serum albumin (BSA) at 10 μ M and cytochrome c at 5 μ M in pH 7.4 PBS to reduce unspecific binding. Molecular samples were prepared in the running buffer (PBS, pH 7.4 supplemented with 20% DMF) and manually injected. The complementary DNA oligomers (intermediate strands: Zip1*-ZipI, Zip2*-ZipII, Zip3*-ZipIII) were subsequently introduced at 200 nM (200 μ L) in the running buffer. Hybridization of the intermediate strands was followed by the injections of IgG–DNA conjugates (anti-CD19IgG-ZipI*, anti-CD90IgG-ZipII and anti-HcBIgG-ZipIII*) at 50 nM. Before the laser desorption, in the case of the cellular experiment, the splenocyte sample injections (5 \times 10⁶ cells/mL) were performed following the molecular construction. These injections started at 80 μ L/min to avoid the sedimentation of cells in the microfluidic tubing and were reduced to 30 μ L/min when cells arrived on the chip in order to minimize the shear stress and favor the capture. Two successive injections of cells were realized. Specific capture of the cells was followed using a microscope under x4 or x10 magnification and registered by a camera (Infinity2-3C, Lumenera). To induce desorption, the laser source was manually introduced between camera and prism and the flow rate was increased to 100 μ L/min. Laser spot was displaced at 10-200 μ m/s which prevent gold surface damaging. Cell recovering was not attempted in these experiments. For the second cell capture experiment, all the biochip preparation steps were performed in the same way. At the end, the biochip was regenerated by 0.1 M NaOH solution (2/3 min), washed by deionized water and dry under argon stream. The microfluidic system was cleaned with 2% commercial bleach during 30 min then washed by 1% SDS and deionized water. All experiments were performed in a dark room at room temperature (25°C).”

3.6 SPRi data analysis and images treatments

The SPRi data were acquired using a home modified SPRi-ViewL3.1.2 software (Horiba Scientific-GenOptics). The acquisition of reflectivity signal, registered with pike F-145B camera started once the cytochrome c injection was completed and the base line stabilized. Reference images were taken at the beginning of each injection to highlight each step of the experiment. The reflectivity values were averaged for each probe family and plotted in time axis after signal correction. Indeed, each SPRi averaged signal was rectified by the R signal subtraction (the reference probe) in order to eliminate the general bulk solution index shift (raw data not shown). The SPRi differential images, the cells images and movies were obtained by contrast optimization in the image treatment software (ImageJ v1.43u, National Institutes of Health, USA).

3.7 Images analysis for cell density quantification

In order to quantify the capture/release and second capture efficiencies, microscope images of the cells were analyzed using ImageJ (ImageJ v1.43u, National Institutes of Health, USA). Color images were converted to gray scale images and a bandpass filter was applied. The number of cells was determined using the “Particles Analysis” ImageJ plugin. The surface of each analyzed area was calculated in order to obtain the surface cell densities. These analyses were performed on 2 to 4 replicates to evaluate the dispersion of the results. The results are presented in the following histogram (figure 4).

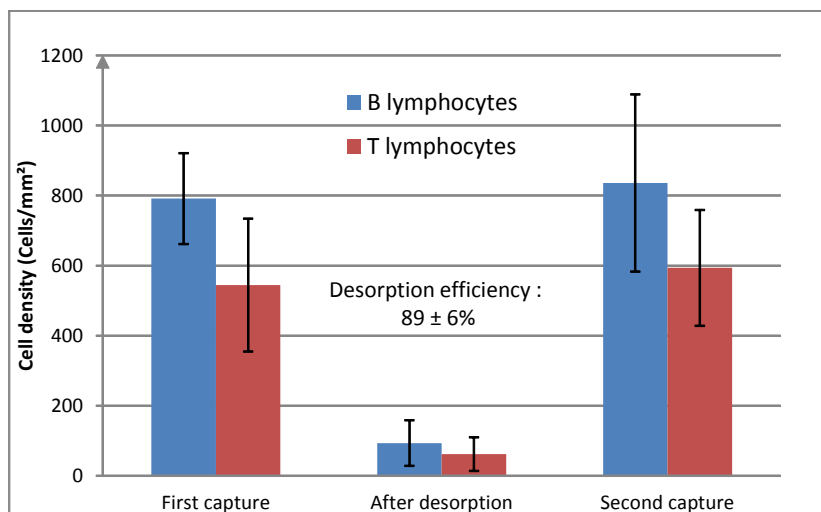


Figure 4. Capture and desorption efficiencies for B- and T- lymphocytes

Error bars represent the standard deviation of the cell densities between replicates. The cell desorption efficiency is about $89 \pm 6\%$ for both cell types. The desorption and the second capture rates were calculated by taking into account only the desorption areas. Nonetheless, in these areas, the second capture step seemed to be slightly more efficient than during the first run. This is probably due to the intrinsic variability in capture efficiency.

3.8 Heat resistance of cells

In order to check the impact of our heating treatment on cells, we set up an experiment to heat a large amount of splenocytes allowing statistically significant viability measurements. Experimental conditions were chosen as close as possible to the real heating treatment. To obtain a rapid increase of temperature to 65°C , an Indium Tin Oxide (ITO) one side coated microscope glass slide (Aldrich) was used. The heating effect was obtained by applying a voltage to the ITO layer between two parallel electrodes. The temperature evolution of the glass side was measured in real-time and controlled by an adjustable power supply monitored by a thermo-regulation Labview software.

Primary splenocytes were collected as described in 3.1 and resuspended in RPMI medium at the concentration of $2.0 \cdot 10^6$ cells/mL (suspension 1). Two series of viability measurements by Vi-Cell XRcell viability analyzer (Beckman Coulter) were performed (figure 5) using $100 \mu\text{L}$ of cells per serie (suspension 1). For the “no heating” condition, the sample of cell suspension was spread on the glass slide side and collected by a gentle rinsing step achieved with $1,9 \text{ mL}$ of RPMI medium. For the “heating” condition, the sample was heated to 65°C for 3 seconds and collected by the same rinsing step. Results are presented on the graph below (figure 5), the histograms show the viability measurements for each condition: respectively 91% and 75%. Errors bars represent the standard deviation obtained for three independent measurements (7%).

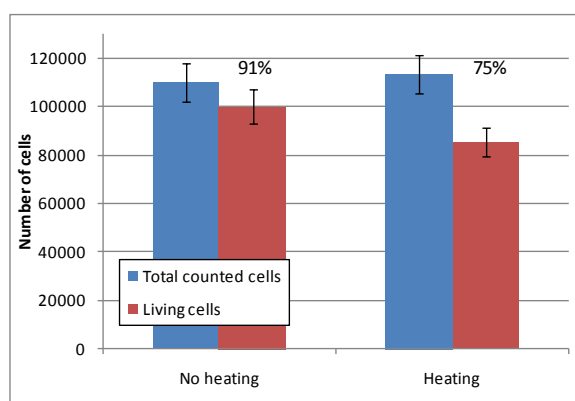


Figure 5. Cell counting and viability measurements for the non-heated and the heated spread samples.

The comparison between the two experiments shows that the mortality specifically induced by the heating treatment does not exceed 16%. As in the real experiment conditions the laser heating is more localized and shorter, cell viability should be even less affected.

4 References

- 1 T. Livache, A. Roget, E. Dejean, C. Barthet, C. Bidan, R. Teoule, *Nucleic Acids Res.* **1994**, *22*, 2915-2921.
- 2 P. Mailley, A. Roget, T. Livache, In E. Palecek, F. Scheller, and J. Wang editors, *Electrochemistry of Nucleic Acids and Proteins*, Vol. 1 of *Perspectives in Bioanalysis*, Elsevier. **2005**, pp297-330.
- 3 P. Guedon, T. Livache, F. Martin, F. Lesbre, A. Roget, G. Bidan, G.; Y. Levy, *Anal. Chem.* **2000**, *72*, 6003-6009.
- 4 C. M. Niemeyer, T. Sano, C. L. Smith, C. R. Cantor, *Nucleic Acids Res.* **1994**, *22*, 5530-5539.
- 5 X. N. Li, Z. W. Du, Q. Huang, J. Q. Wu, *Neurosurgery.* **1997**, *40*, 1250-1258; discussion 1258-1259.
- 6 D. L. Dexter, J. A. Barbosa, P. N. Calabresi, *Cancer Res.* **1979**, *39*, 1020-1025.
- 7 T. W. Grunt, C. Somay, A. Ellinger, M. Pavelka, E. Dittrich, C. Dittrich, *J. Cell Physiol.* **1992**, *151*, 13-22.
- 8 J.-B. Fiche, A. Buhot, R. Calemczuk, T. Livache, *Biophys. J.* **2007**, *92*, 935-946.
- 9 H. Urakawa, P. A. Noble, S. El Fantroussi, J. J. Kelly, D. A. Stahl, *Appl. Environ. Microbiol.* **2002**, *68*, 235-244.
- 10 A. E. Pozhitkov, R. D. Stedtfeld, S. A. Hashsham, P. A. Noble, *Nucleic Acids Res.* **2007**, *35*, 70.
- 11 J. Fuchs, D. Dell'Atti, A. Buhot, R. Calemczuk, M. Mascini, T. Livache, *Anal. Biochem.* **2010**, *397*, 132-134.
- 12 E. Kretschmann, H. Raether, Radiative Decay of Non Radiative Surface Plasmons Excited by Light. *Zeitschrift Fur Naturforschung Part a-Astrophysik Physik Und Physikalische Chemie* **1968**, *A23*, 2135-2136.